Pharmaceutical Research, Vol. 11, No. 1, 1994

Research Article

Intracellular Visualization of Ampicillin-Loaded Nanoparticles in Peritoneal Macrophages Infected *in Vitro* with *Salmonella typhimurium*

Huguette Pinto-Alphandary,[1,4] Olivier Balland,[1] Michel Laurent,[2] Antoine Andremont,[3] Francis Puisieux,[1] and Patrick Couvreur[1]

Received March 17, 1993; accepted June 27, 1993

Intracellular targeting of ampicillin by means of polyisohexylcyanoacrylate (PIHCA) nanoparticles was studied in murine peritoneal macrophages infected with *Salmonella typhimurium*. The intracellular distribution of actively endocytosed nanoparticles was visualized by transmission electron microscopy and confocal microscopy. Nanoparticles were either isolated or closely associated with bacteria within phagosomes or phagolysosomes. Thus the potential of ampicillin-loaded nanoparticles in targeting of intracellular bacteria is demonstrated. Consequently, ampicillin, which usually penetrates into cells at a low level, is directly carried in, when loaded on nanoparticles, and brought into contact with intracellular bacteria.

KEY WORDS: nanoparticles; ampicillin; peritoneal macrophage; *Salmonella typhimurium;* intracellular infection.

INTRODUCTION

Facultative intracellular bacteria including *Brucella, Listeria, Mycobacteria,* and *Salmonella* species are able to survive and multiply mainly within phagocytic cells of the reticuloendothelial system, constituting reservoirs of pathogenic bacteria. In *Salmonella* infections, the invading agent inhibits predominantly phagosome–lysosome (P/L) fusion (1,2) and secondarily resists antimicrobial actions when residing in P/L (3). Although often used to treat intracellular infections, β-lactam antibiotics have a low intracellular uptake in phagocytic cells (4) and do not diffuse through the lysosomal membrane (5).

Loading antibiotics on colloidal carriers is a promising approach to overcoming the limits of classical antimicrobial therapy. Indeed, the lysosomotropic properties of these carriers have been used to transport and concentrate various drugs into cells (6–8,9). For *S. typhimurium,* liposomal encapsulation (10–12) or nanoparticle loading (12,13) has been developed to enhance the intracellular delivery of antibiotics. The intracellular location of such antimicrobial-loaded liposomes has been studied by microscopic examination (14,15). We have chosen to use ampicillin–polyisohexylcyanoacrylate (PIHCA) nanoparticles instead of ampicillin–liposomes because they are more stable and more efficient in murine salmonellosis (12,13). Tissue targeting (liver and spleen) has been clearly demonstrated, but the intracellular trafficking events of nanoparticles in infected target cells (macrophages) are unknown. The lysosomotropic character of nanoparticles has been well documented in uninfected fibroblasts (7,16), but a detailed ultrastructural investigation of the intracellular distribution of nanoparticles has never been performed. Thus, the aim of the present study was to analyze the cellular targeting of nanoparticle ampicillin toward compartments infected with *S. typhimurium.* Ultrastructural studies by electron microscopy allowed us to localize the nanoparticles within intracellular compartments and determine whether they can reach phagosomes and target the bacteria that reside therein. Complementary observations by confocal laser microscopy were performed using double fluorescent labeling with fluorescent nanoparticles and immunolabeled fluorescent *Salmonella.*

MATERIALS AND METHODS

Ampicillin-Loaded Nanoparticles

Unlabeled ampicillin-nanoparticles used for transmission electron microscopy were prepared by emulsion polymerization of isohexylcyanoacrylate (IHCA) monomer as described by Couvreur *et al.* (17) and Henry-Michelland *et al.* (18). IHCA monomer was obtained from Sopar (Sart-Dames, Avelines, Belgium), and ampicillin trihydrate from Negma (Buc, France). The aqueous polymerization medium (10 mL), adjusted to pH 2.8 with HCl, contained 1% dextran

[1] Laboratoire de Pharmacie Galénique, CNRS, URA 1218, Faculté de Pharmacie, 92296 Châtenay-Malabry Cedex, France.
[2] Service d'Imagerie cellulaire, URA 1116, Bât. 441, Université Paris-Sud, 91405 Orsay Cedex, France.
[3] Laboratoire d'Ecologie microbienne, Institut Gustave Roussy, 94805 Villejuif Cedex, and Laboratoire de Microbiologie, Faculté de Pharmacie, 92296 Châtenay-Malabry Cedex, France.
[4] To whom correspondence should be addressed.

0724-8741/94/0100-0038$07.00/0

70 (Fluka, France), 5% glucose, and 2 mg ampicillin/mL. The IHCA monomer (100 μL) was then added; after 6 hr of polymerization, the suspension was adjusted to pH 7 with 0.1 *M* NaOH. The amount of ampicillin associated with polyisohexylcyanoacrylate (PIHCA) nanoparticles was 90 ± 4% as determined by HPLC (19), i.e., 18 mg ampicillin/100 mg PIHCA nanoparticles. The diameter of the ampicillin-nanoparticles, estimated by laser light scattering (Nanosizer Coulter N4MD, Coultronics, France), was 220 ± 25 nm (n = 4). Aliquots (1 mL) of ampicillin-nanoparticles were lyophilized using 5% glucose as cryoprotector. For each experiment, an aliquot was reconstituted by adding 1 mL distilled water; it did not change the size and the drug content of ampicillin-nanoparticles.

Fluorescent ampicillin-nanoparticles used for optical confocal microscopy were prepared as follows: Ampicillin-loaded nanoparticles were labeled using fluorescein isothiocyanate-dextran 70 (FITC-dextran 70, Sigma, France) instead of dextran. Their size was 120 ± 30 nm (n = 4). Free fluorescent dextran was eliminated by ultracentrifugation on preformed sucrose gradients (40 and 20%, w/v; 2, 2.5, and 1 mL sample, respectively) at 150,000 *g* for 1 hr at 10°C in an ultracentrifuge (Beckman). Fluorescent dextran remained in the upper phase. The band of fluorescent ampicillin-nanoparticles was recovered by puncturing the tube at the 20–40% interface. Polymer concentration was measured by turbidimetry at 550 nm (Lambda 5 spectrophotometer, Perkin–Elmer) after determination of the standard curve. This value was corrected (10%) for overlapping of the optical absorption due to the fluorescent derivative. An $OD_{550\ nm}$ of 0.8 corresponded to a concentration of 10 mg of PIHCA/mL.

Bacterial Strain

Salmonella typhimurium C5 strain was obtained from Institut Pasteur (Paris, France). Bacteria were grown in BHI broth (Difco, France) at 37°C, harvested in the logarithmic phase, and washed twice in phosphate-buffered saline (PBS). Opsonization was obtained after 30 min of incubation at 37°C with a subagglutinating concentration of anti-*Salmonella* serum (O: 4,5; Diagnostics Pasteur, France). The opsonized bacteria (10^9/mL) were washed in PBS and adjusted to 2×10^7/mL in the culture medium. Bacterial concentrations were determined by optical density at 620 nm and by counting cells in a Salumbeni chamber (Preciss, France) and confirmed by counting colony-forming units on agar plates.

Macrophage Monolayers

Resident murine peritoneal macrophages were harvested from OF1 mice (age, 6 to 8 weeks; Iffa-Credo, Les Oncins-l'Arbresle, France) by peritoneal lavage with Hank's balanced salt solution (HBSS; GIBCO Laboratories, France). Cells were washed and resuspended at a concentration of 10^6/mL in RPMI 1640 supplemented with 10% fetal calf serum (FCS). For electron microscopy, 2 mL of the macrophage suspension was placed in 35-mm tissue culture dishes (Falcon, Becton Dickinson Labware, U.S.A.). For confocal microscopy, the macrophage suspension was placed in 24-well culture plates (0.5 mL/well containing a 13-mm coverslip). The monolayers were incubated for 2 hr at 37°C in a 5% CO_2 incubator and then washed with fresh culture medium to remove nonadherent cells and incubated for additional 2 days at 37°C in a 5% CO_2 incubator.

Incubation of Macrophages with Unlabeled Ampicillin-Nanoparticles

The experimental conditions were the same as described above. For electron microscopy studies, uninfected macrophages (2×10^6 cells/dish) were incubated at 37°C with unlabeled ampicillin-nanoparticles (10 μg of PIHCA/mL, 15 min; and 20 μg PIHCA/mL, 90 min and 14 hr). These incubation times were chosen taking into account the slow degradation rate of PIHCA.

Infection of Macrophages and Treatment with Unlabeled Ampicillin-Nanoparticles

For electron microscopy studies, macrophage monolayers (2×10^6 cells/dish) were infected with opsonized bacteria (cell-to-bacteria ratio, 1:10) for 30 min at 37°C in a 5% CO_2 incubator. Under these conditions, the entire monolayer was infected.

After infection with *S. typhimurium*, macrophages were rinsed three times with PBS and treated immediately with ampicillin-nanoparticles at an ampicillin concentration of 2 μg/mL (corresponding to 10 μg of PIHCA/mL), in the presence of gentamicin (10 μg/mL). Incubation was carried out for 90 min and 3 hr, to visualize the nanoparticles well before excessive degradation. Persistence of the ampicillin–nanoparticle association and intracellular release of ampicillin from these nanoparticles have been reported elsewhere (20). The cytotoxicity of PIHCA nanoparticles was determined previously [dose killing 50% of peritoneal macrophages (DL_{50}) was 100 μg/mL after 12 hr of incubation]. The cytotoxicity of drug-free nanoparticles and nanoparticle degradation products on *S. typhimurium* was examined (data not shown); no antimicrobial effect was detected. This is not surprising since the nanoparticle degradation product polyisohexylcyanoacrylic acid is a very hydrophilic compound unable to diffuse into the bacteria. Gentamicin (Sarbach, France) added to the incubation medium prevents the division of extracellular bacteria. In preliminary experiments we showed that this concentration does not affect the number of intracellular bacteria.

Confocal Laser Scanning Microscopy

Uninfected peritoneal macrophages (5×10^5 cells/well) adhering to 13-mm coverslips were incubated with ampicillin-nanoparticles labeled with FITC-dextran 70 (20 μg of PIHCA/mL) for 90 min at 37°C. Cells were treated, as described below, without immunofluorescence labeling.

Peritoneal macrophages (5×10^5 cells/well) adhering to 13-mm coverslips were infected with opsonized *S. typhimurium*, as described above, and rinsed three times with PBS. The macrophages were immediately treated with fluorescent ampicillin-nanoparticles (100 μg of PIHCA/mL) in the presence of 10 μg/mL gentamicin for 90 min at 37°C. Indirect immunofluorescence was then used to label bacteria. The macrophages were submitted to a procedure described elsewhere (21) and modified as follows. They were fixed for 30 min at 4°C with 2.5% *p*-formaldehyde in PBS containing 2 m*M* $MgCl_2$ and 5 m*M* $CaCl_2$ (solution A) and washed with

PBS. After 10 min of neutralization with 50 m*M* NH_4Cl in PBS and washing, cells were permeabilized for 5 min with 0.1% Triton X-100 in solution A and washed with PBS. Nonspecific sites were blocked with PBS containing 3% bovine serum albumin (BSA; Sigma, France) during 30 min at 20°C. Macrophages were incubated for 1 hr at 37°C, with a 1:100 dilution of the first antibody (rabbit anti-*Salmonella* serum) in PBS + 0.5% BSA (solution B). After washing, a 1:200 dilution of the secondary antibody in solution B was added (Texas red-conjugated goat anti-rabbit IgG; Jackson, France) and incubation was carried on for 1 hr at 37°C. Coverslips were then rinsed in PBS and mounted in antifading solution AF1 (Citifluor Ltd, England). Optical sectioning was performed with a MRC-600 confocal laser scanning microscope (Bio-Rad, Ivry, France) equipped with a 25-mW argon-ion laser and two detector channels allowing simultaneous confocal imaging of double-labeled material. For double-labeling experiments, pairs of dyes (FITC and Texas red derivatives) were excited using the 514-nm green line from the argon-ion laser. Thanks to an appropriate combination of filters, fluorescence emission was divided into yellow/green (520- to 550-nm) and red (600-nm and above) components, which were directed through different confocal apertures to the two separate photomultipliers. Since overlapping of FITC and Texas red emission spectra prevents any perfect separation, computer software was written to correct for this bleed-through effect.

Quantitative estimation of the bacteria which were superimposed with nanoparticles was done by counting the number of bacteria displaying both red and yellow-green fluorescences and expressing it as a percentage of the total number of bacteria.

Transmission Electron Microscopy

Enzymatic hydrolysis (22) of PIHCA in unlabeled ampicillin-nanoparticles (1 mg of polymer/mL) was induced by incubation for 12 hr in the presence of 30 IU esterase (carboxylic ester hydrolase; EC 3.1.1.1; Sigma, France) at 37°C in PBS, pH 7.4. These bioeroded nanoparticles were compared with a control sample incubated under the same conditions without enzyme. Nanoparticles were negatively stained by floating the grids coated with a Formvar film (Fullam, France) in 2% uranyl acetate.

The behavior of ampicillin-nanoparticles in macrophages was examined by positive staining on ultrathin sections according to the following procedure. Macrophages were incubated with ampicillin-nanoparticles or infected with *S. typhimurium* and then treated with ampicillin-nanoparticles. The cells were fixed in 2.5% glutaraldehyde (Sigma, France) in 0.1 *M* cacodylate buffer (5 m*M* $CaCl_2$, 5 m*M* $MgCl_2$, and 0.1 *M* sucrose, pH 7.2) overnight at 4°C and then washed; they were postfixed with 1% osmium tetroxide (Comptoir Lyon Alemand Louyot, France) in the same buffer for 1 hr at 20°C and then washed. Macrophages were gently scraped with a cell scraper and concentrated in 2% agar. The specimens were then treated with 2% uranyl acetate in Michaelis buffer, pH 6.0, for 1 hr at 20°C (23). The material was dehydrated through graded series of ethanol solutions, followed by embedding in Epon (Fullam, France). Ultrathin sections were double-stained with 2% uranyl acetate and then 0.2% lead citrate. When ruthenium red (Taab, France) was used, the dye was added (1%) from fixation to dehydratation. After double-staining of ultrathin sections exposed to ruthenium red, the contrast of the nanoparticles,

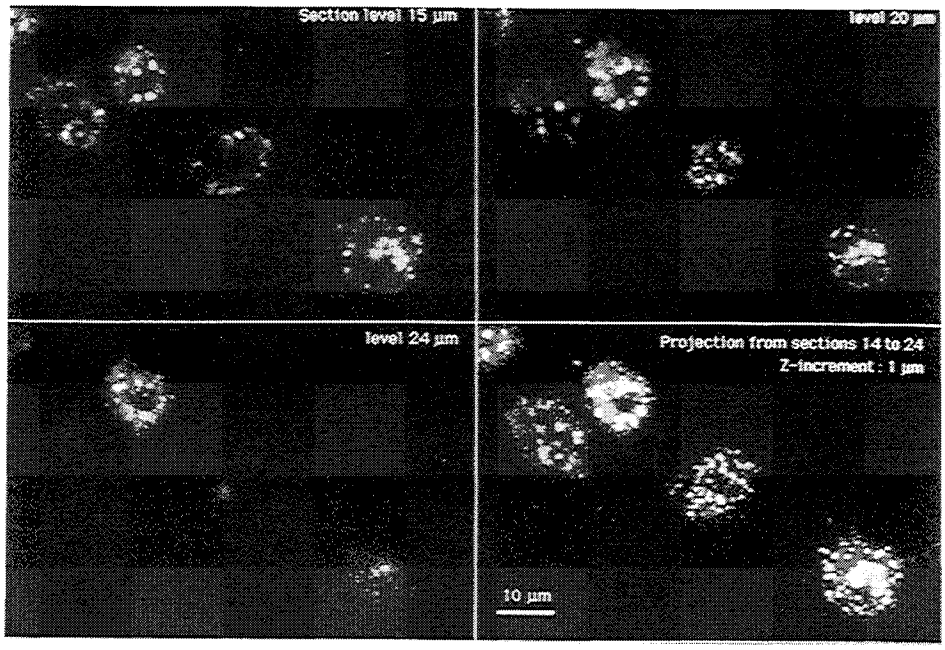

Fig. 1. Confocal micrographs of ampicillin-nanoparticles endocytosed by mouse peritoneal macrophages. Cells were incubated for 90 min at 37°C with ampicillin-nanoparticles (20 µg of PIHCA/mL) labeled with FITC-dextran 70. A set of 25 optical sections obtained at 1-µm intervals was acquired with a Bio-Rad MRC-600 confocal microscope (excitation with the 488-nm line from an argon-ion laser). Three individual optical sections are shown, as well as the maximum brightness projection image of a selected part of the complete 3-D data set.

which usually shows a tenuous outline, and that of all cellular components were greatly enhanced.

Observations were made under a transmission electron microscope (EM 301-Philips) operating at 80 kV.

RESULTS

Size of Unlabeled and of Fluorescent Ampicillin-Nanoparticles

The size of unlabeled ampicillin-nanoparticles was 220 ± 25 nm and that of fluorescent ampicillin-nanoparticles was 120 ± 30 nm. This difference might be due to the size of the "pseudo-micelles" during the polymerization. Classically, when a surfactant is used, the size of the particles depends on the size of the micelles obtained (24). Since dextran is not a surfactant, the "nuclei" of polymerization are considered pseudo-micelles by analogy with micelles formed by surfactants during the emulsion polymerization process. FITC-dextran could change the characteristics of those nuclei of polymerization.

The size and drug content of fluorescent nanoparticles were not modified after ultracentrifugation. The isolated fluorescent ampicillin-nanoparticles recentrifuged through an identical sucrose gradient did not release dextran, suggesting a tightly bound interaction with the polymer.

Endocytosis of Ampicillin-Nanoparticles by Macrophages

In a preliminary experiment, the absence of penetration of free FITC-dextran 70 was observed at the concentrations used. Therefore, fluorescent dextran was revealed to be a good marker for ampicillin-nanoparticles. After 5 min of incubation, the nanoparticles were located mainly at the periphery of the cells (data not shown). Yet the amount of endocytosis was low under such conditions. Increasing the incubation time up to 90 min resulted in a different pattern of intracellular fluorescence (Fig. 1). On one hand, projection of the three-dimensional (3-D) data showed that FITC fluorescence remained essentially vesicular. Thus, ampicillin-nanoparticles, trapped mainly in endocytic vacuoles, were mostly nondegraded. On the other hand, fluorescent grains extended over the cytoplasm. Optical section examinations gave insight into the localization of labeled nanoparticles: their 3-D distribution in the cell demonstrated that they penetrated the macrophages by an endocytic way.

Transmission electron microscopy was used in a preliminary experiment to examine the aspect of bioeroded ampi-

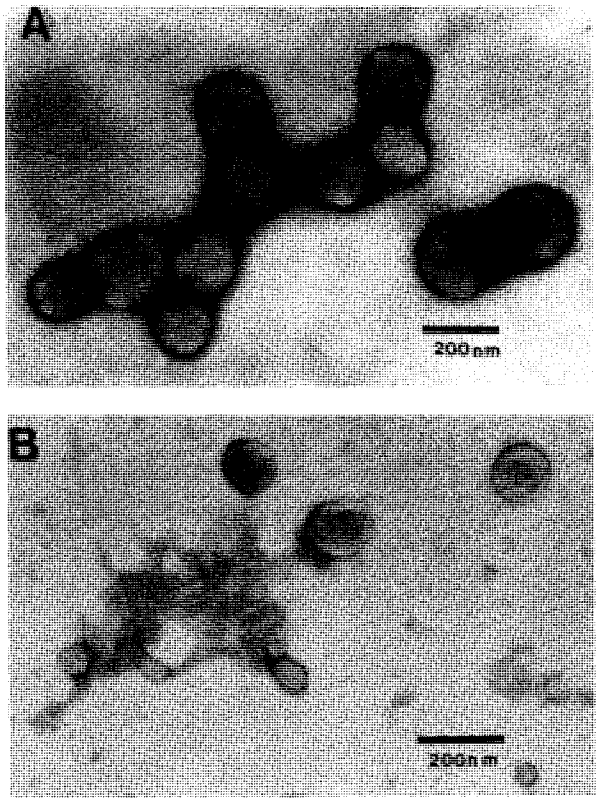

Fig. 2. Electron micrographs after negative staining of ampicillin-nanoparticles. Incubation at 37°C for 12 hr in PBS: control (A); with esterase (B). Degradation was visualized by the release of electron-dense material.

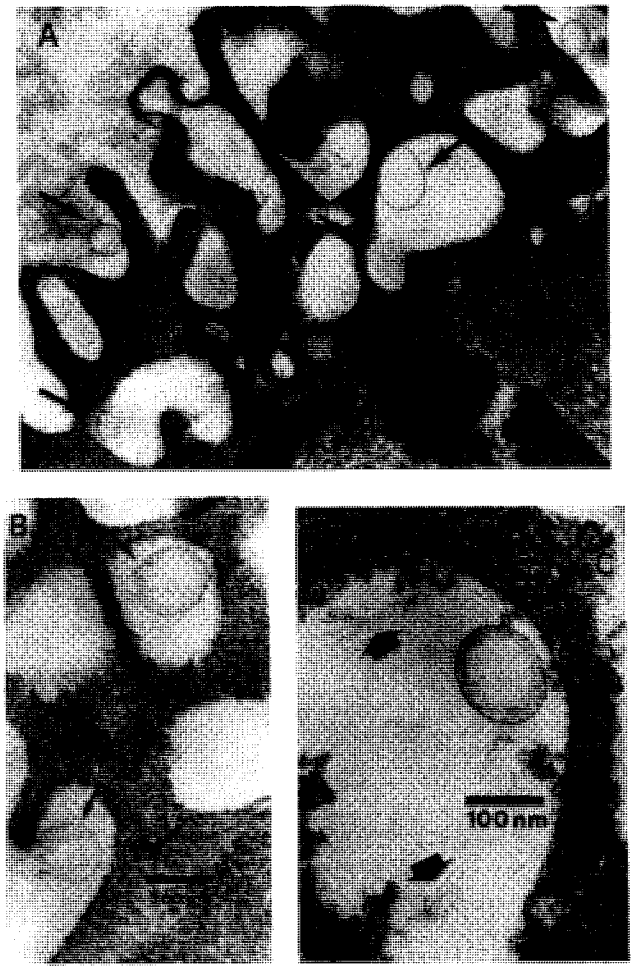

Fig. 3. Transmission electron micrographs of peritoneal macrophages incubated with ampicillin-nanoparticles. (A) After 15 min of incubation (10 μg of PIHCA/mL): nanoparticles adhering to the plasma membrane, before their engulfment by pseudopods (arrows). (B) After 90 min of incubation (20 μg of PIHCA/mL): arrows indicate nanoparticles enclosed in endocytic vacuoles. (C) After 14 hr of incubation (20 μg of PIHCA/mL): enzymatic erosion of nanoparticles (thick arrows indicate degraded material).

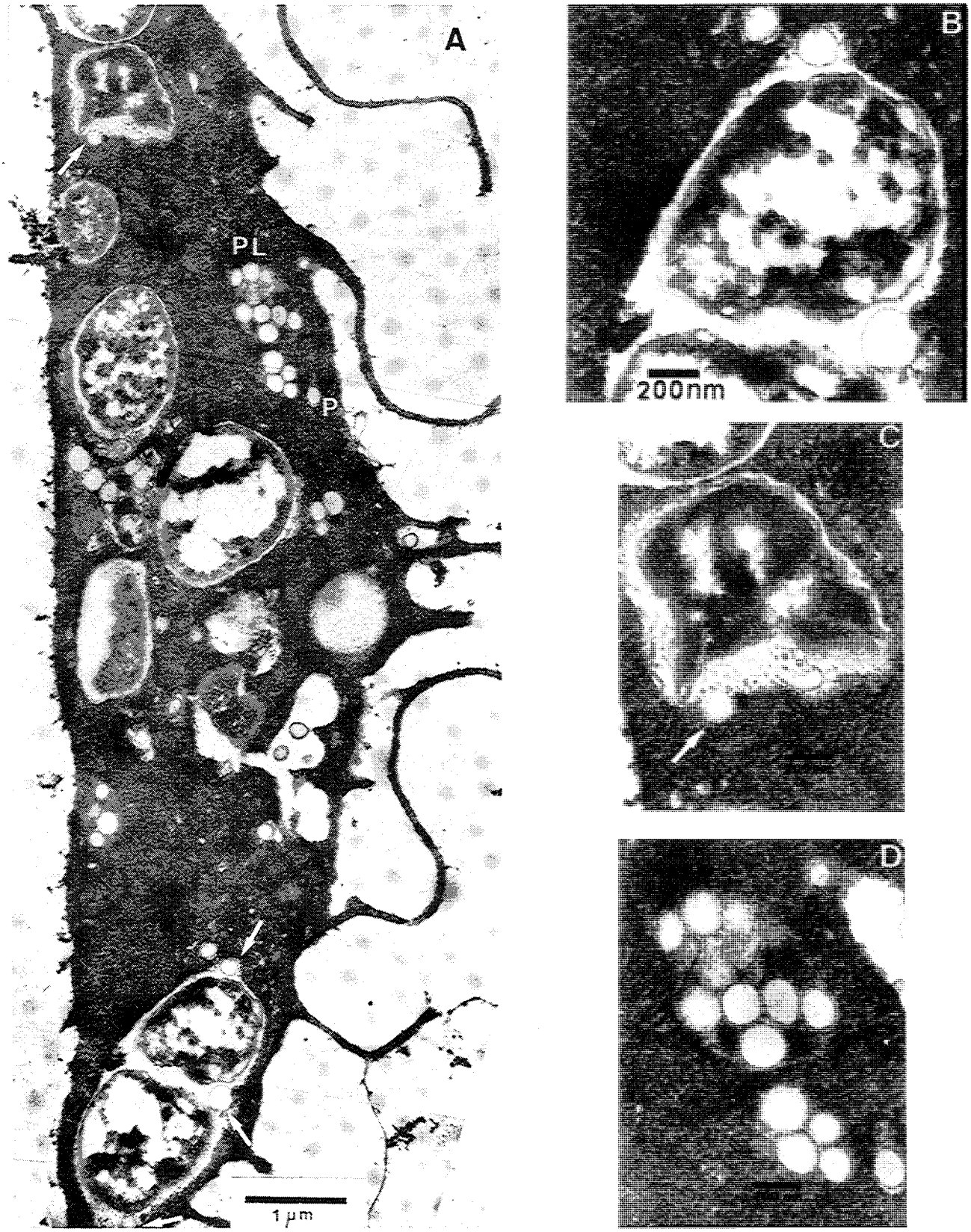

Fig. 4. Localization of ampicillin-nanoparticles in peritoneal macrophages infected with *S. typhimurium*. (A–D) After infection (30 min) and rinsing three times with PBS, macrophages were treated with ampicillin-nanoparticles (10 µg of PIHCA/mL) in the presence of gentamicin (10 µg/mL) for 90 min. The electron contrast was enhanced with ruthenium red. (B–D) Details of A. (A) Nanoparticles isolated or grouped in phagosomes (P) or in phagolysosomes (PL) (detail in D). Many nanoparticles (white arrows) were juxtaposed with bacteria in the same compartment. (B) A dividing bacterium close to nanoparticles.

cillin-nanoparticles. Unlabeled ampicillin-nanoparticles were incubated in the presence of esterase and observed by negative staining (Fig. 2). After enzymatic attack, nanoparticle size was reduced and electron-opaque material was detached from the nanoparticles; further, it was polymeric (partly degraded polycyanoacrylate and nonbiodegradable dextran). This observation suggested that, for long incubation times, the nanoparticles would become difficult to identify, especially after digestion by lysosomal esterases.

Transmission electron micrographs (Fig. 3A) showed that unlabeled ampicillin-nanoparticles were rapidly endocytosed by the macrophages. The plasma membrane formed numerous pseudopods engulfing nanoparticles. Nanoparticles were identified by their size (diameter nearly 200 nm or less in ultrathin sections), by their spherical shape, with a characteristic, moderately electron-dense "coat," and by their electron transparent content. All these criteria allowed the distinction of nanoparticles from cellular organelles; moreover, the latter contained particulate, granular, or dense material and were limited by a double-layered membrane in direct contact with the cytoplasm. Endocytic vesicles were observed to contain intact nanoparticles (Fig. 3B) or nanoparticles in the process of degradation (Fig. 3C), generally characterized by a gray-tinted envelope.

Treatment of Infected Macrophages with Ampicillin-Nanoparticles

Ultrastructural studies allowed us to go further in understanding the vectorization mechanism at the level of cell compartments. Transmission electron microscopy of infected peritoneal macrophages treated with unlabeled ampicillin-nanoparticles allowed us to visualize nanoparticles inside the same compartments as bacteria (Figs. 4 and 5). This observation confirms the principal aspect of the expected targeting of the antibiotic. The degradation of bacteria (Fig. 4C) suggested the presence of lysosomal enzymes and consequently the phagolysosomal nature of the compartment. The observation of grouped nanoparticles (Fig. 4D) with electron-opaque material, probably originated from polymeric degradation, indicated that this vacuole was a phagolysosome. Fusion of phagosomes with lysosomes took place between about 30 min and 1 hr. Some bacteria were observed to be in the process of degradation in the same vacuole as nanoparticles. However, numerous isolated or grouped particles were localized in compartments apparently free of bacteria (Figs. 4A and D and 6). Formation of these clusters in the same vesicles (Fig. 4D) was probably derived from the fusion of phagocytic vacuoles and, possibly, of lysosomes.

The main purpose of the confocal microscopy was to obtain a general view of the distribution of nanoparticles and bacteria in macrophages and to realize numerous observations of this distribution. This method was used to quantify the targeting of ampicillin-nanoparticles toward the infected intracellular sites. Fluorescent labeling of ampicillin-nanoparticles and *S. typhimurium* probed with FITC-dextran and Texas red-coupled antibody, respectively, allowed us to examine their comparative intracellular distribution (Fig. 7). To increase the fluorescence detection level, fluorescent ampicillin-nanoparticles were added to infected macrophages at a concentration five times higher than in the

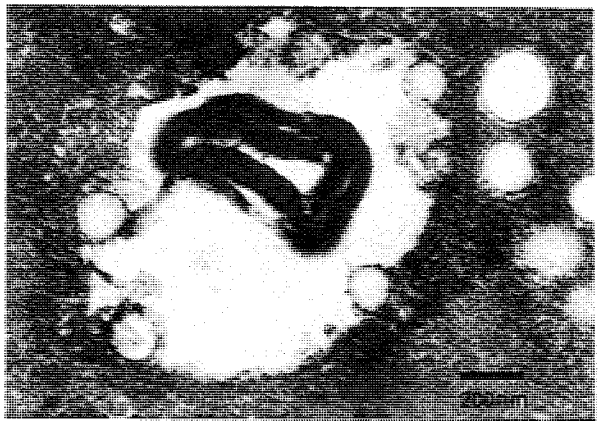

Fig. 5. Experimental conditions similar to those for in Fig. 4. Nanoparticles are visible inside and outside a phagolysosome and a bacterium is seen to be disintegrated.

electron microscopy experiments with unlabeled ampicillin-nanoparticles. The intracellular localization of the bacterial material was proved by examination of the individual optical sections (Fig. 7). After 90 min of incubation (Fig. 7), red-channel confocal images showed the presence of both intact bacteria and bacterial fragments, providing evidence of partial disintegration of *S. typhimurium*. The percentage of intracellular bacteria in contact with the nanoparticle fluorescence was estimated. From all the optical section observations, about 75% of fluorescent *Salmonella* (intact or degraded) could be superimposed with the nanoparticle fluorescence. However, confocal microscopy did not allow us to distinguish nanoparticles and bacteria in the same vacuole and the resolution was limited by the thickness of the optical plane (about 500 nm). Consequently, this method was used to obtain general views of the distribution of nanoparticles and bacteria.

The green-channel images were clearly dependent on the duration of the endocytosis process. For 90 min of incubation (Fig. 7), FITC fluorescence was mainly vesicular. In contrast, it became very diffuse after 3 hr of endocytosis, as a consequence of the progressive degradation of nanoparticles (data not shown). Because of this diffusion, the obser-

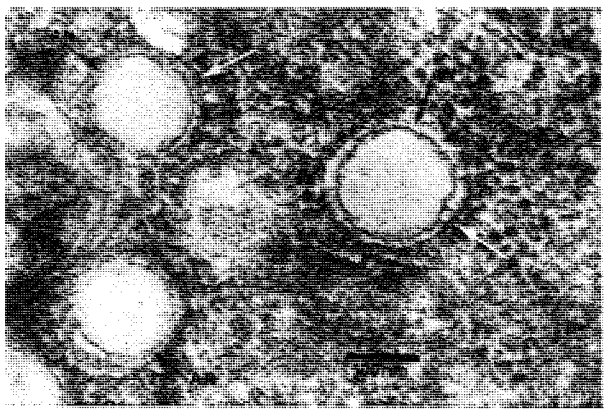

Fig. 6. Experimental conditions similar to those in Fig. 4. After 3 hr of incubation, nanoparticles (indicated by AN and arrows) were clearly internalized in endocytic vacuoles with a double-layered membrane (white arrows) derived from the plasma membrane.

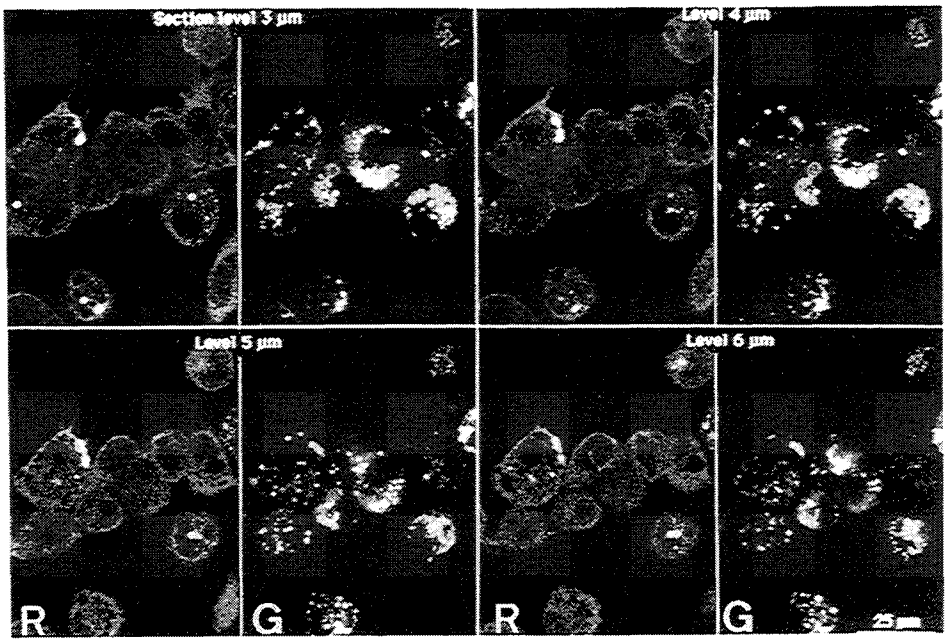

Fig. 7. Confocal micrographs of peritoneal macrophages infected with *Salmonella typhimurium* and then treated with ampicillin-nanoparticles (90 min of incubation, 100 µg of PIHCA/mL, in the presence of 10 µg/mL of gentamicin). Nanoparticles were labeled with FITC-dextran 70 and bacteria by an indirect immunofluorescence method with a secondary Texas red-coupled antibody. Texas red and FITC fluorochromes were excited simultaneously using the 514-nm laser line. The left half of the micrographs corresponds to the red-channel images (R). The associated green-channel images (G) are shown in the right half. The figure corresponds to the optical sections collected at 1-µm intervals in the two channels. This sequence demonstrates the intracellular localization of the bacterial material and degraded bacteria.

vations might be limited for long incubations, contrary to bacteria, whose labeling was much more stable with Texas red.

DISCUSSION

Confocal microscopy and transmission electron microscopy provide information on the intracellular traffic of ampicillin-nanoparticles in peritoneal macrophages, particularly with regard to the possibility to observe *S. typhimurium* within macrophage compartments.

FITC-dextran was found to be a good labeling probe of ampicillin-nanoparticles in short-term incubation experiments (90 min). Indeed, dextran has been observed to be tightly bound to the polymeric structure (25), and PIHCA nanoparticles are enzymatically degraded at a slow rate (8). The intracellular distribution of ampicillin-nanoparticles was visualized in vesicular compartments of macrophages and was consistent with that in previously published experiments using propidium iodide-labeled polyisobutylcyanoacrylate nanoparticles in L929 fibroblasts (16).

In other respects, examination of ultrathin sections by transmission electron microscopy revealed the formation of pseudopods at the cell membrane, endocytic vacuoles, and accumulation of nanoparticles within phagosomal and phagolysosomal compartments. The localization of nanoparticles in phagolysosomal vacuoles suggested that there was fusion between vacuoles containing nanoparticles and primary lysosomes; this is in agreement with the well-known lysosomotropic character of the carrier (7). Thus, by electron microscopy and confocal microscopy, the data clearly demonstrated that active uptake of ampicillin-nanoparticles by peritoneal macrophages.

Transmission electron microscopy allowed us also to observe the colocalization of ampicillin-nanoparticles and bacteria and demonstrated the feasibility of targeting bacteria by means of nanoparticles. In infected macrophages, bacteria undergoing degradation could be observed (Figs. 4 and 5). However, after 90 min of incubation, it was not possible to discriminate between the bactericidal effect of the ampicillin-nanoparticles and that of macrophages themselves, which essentially takes place in the first hour following the infection (10).

The frequency with which one nanoparticle and one bacterium were observed by electron microscopy in the same vacuole was estimated on the same ultrathin section. It was found that about 1 to 5% of bacteria could be seen jointly with nanoparticles. However, according to the smaller diameter of the nanoparticles (0.22 µm) compared to the size of the bacteria (2 × 0.5 µm), the probability of observing a nanoparticle and a bacterium together on the same ultrathin section is about 10 times lower than the frequency of a real encounter. Thus, although this event was rarely detected, the real frequency should be notably higher, lending evidence to a significant targeting of ampicillin-nanoparticles toward infecting bacteria.

The inhibition of phagosome–lysosome fusion due to *S.*

typhimurium described elsewhere (1,2) could prevent contact between the bacteria, present mainly in phagosomes, and ampicillin-nanoparticles, present in secondary lysosomes. This mechanism is, thus, supposed to limit partly the intracellular targeting of *S. typhimurium* by nanoparticles and could explain our observations that numerous bacteria were detected inside compartments apparently free of nanoparticles.

Concerning ampicillin release from nanoparticles, it could be, as reported previously, that the drug was liberated after bioerosion of the nanoparticles (24,26). On the other hand, it has been shown that even though pure chemical hydrolysis may occur at high pH levels, the main part of the bioerosion process resulted from the enzymatic degradation through esterases (22). With regard to the diffusion of drug out of intact nanoparticles, it seemed to occur at a very low rate (18,12). Thus, in our model, it was reasonable to consider that the polymer should be essentially degraded intracellularly by lysosomal esterases before the antibiotic could be released to display a significant antimicrobial effect. Moreover, degradation of nanoparticles could be detected within a short time (90 min). In this case, degraded nanoparticles corresponded to the release of electron-dense material.

Incubations for longer times (14 hr) were realized, but as bioerosion progressed, the nanoparticles could not be identified with certainty (Fig. 2B, control) or they were difficult to see (Fig. 3C) since their size was reduced and the polymer was rather solubilized. Consequently, only short incubation times (1–3 hr) allowed unquestionable identification of nanoparticles.

Finally, it is important to note that the eventual toxic effect of the degradation products from nanoparticles on bacteria in the phagolysosomes was not measured under our conditions. However, drug-free nanoparticles have previously shown no antimicrobial effect (20).

In conclusion, the observation of ampicillin-nanoparticles jointly with intracellular bacteria demonstrated that the drug could be concentrated in infected cell compartments inducing a direct *in situ* action by contact of nanoparticles with the bacteria. On the other hand, released ampicillin may also diffuse (5) across lysosomal membranes, to be redistributed through the cell, reaching bacteria located in other compartments. Thus, the antibacterial efficacy may have resulted from both direct targeting of bacteria by ampicillin-nanoparticles and diffusion of the antibiotic from one vacuole to another.

ACKNOWLEDGMENTS

This study was supported by Laboratoires Negma (Buc, France) and the "Réseau Vectorisation" (DRED, Ministère de l'Education Nationale, France). We are grateful to C. Fréhel and C. de Chastellier for fruitful discussions and E. Fattal and F. Forestier for critical reading of the manuscript.

REFERENCES

1. Y. Ishibashi and T. Arai. Specific inhibition of phagosome-lysosome fusion in murine macrophages mediated by *Salmonella typhimurium* infection. *FEMS Microbiol. Immunol.* 64:35–44 (1990).
2. N. A. Buchmeier and F. Heffron. Inhibition of macrophage phagosome-lysosome fusion by *Salmonella typhimurium*. *Infect. Immun.* 59:2232–2238 (1991).
3. M. E. W. Carrol, P. S. Jackett, V. R. Aber, and D. B. Lowrie. Phagolysosome formation, cyclic adenosine 3′:5′-monophosphate and the fate of *Salmonella typhimurium* within mouse peritoneal macrophages. *J. Gen. Microbiol.* 110:421–429 (1979).
4. I. A. J. M. Bakker-Woudenberg, P. de Bos, W. B. van Leeuwen, and M. F. Michel. Efficacy of ampicillin therapy in experimental listeriosis in mice with impaired T-cell-mediated immune response. *Antimicrob. Agents Chemother.* 19:76–81 (1981).
5. C. Renard, H. J. Vanderhaeghe, P. J. Claes, A. Zenebergh, and P. M. Tulkens. Influence of conversion of penicillin G into a basic derivative on its accumulation and subcellular localization in cultured macrophages. *Antimicrob. Agents Chemother.* 31:410–416 (1987).
6. P. Couvreur. Polyalkylcyanoacrylates as colloidal drugs carriers. In *Crit. Rev. Ther. Drug Carrier Sys.* 5:1–20 (1988).
7. P. Couvreur, B. Kante, and M. Roland. Les vecteurs lysosomotropes. *J. Pharm. Belg.* 35:51–60 (1980).
8. P. Couvreur, L. Grislain, V. Lenaerts, F. Brasseur, P. Guiot, and A. Biernacki. Biodegradable polymeric nanoparticles as drug carrier for antitumor agents. In P. Guiot and P. Couvreur, (eds.), *Polymeric Nanoparticles and Microspheres,* CRC Press, Boca Raton, FL, 1986, pp. 27–93.
9. C. R. Alving. Macrophages as targets for delivery of liposome-encapsulated antimicrobial agents. *Adv. Drug Deliv. Rev.* 2:107–128 (1988).
10. J. V. Desiderio and S. G. Campbell. Liposome-encapsulated cephalothin in the treatment of experimental murine salmonellosis. *J. Reticuloendothel. Soc.* 34:279–287 (1983).
11. C. E. Swenson, K. A. Stewart, J. L. Hammet, W. E. Fitzsimmons, and R. S. Ginsberg. Pharmacokinetics and *in vivo* activity of liposome-encapsulated gentamicin. *Antimicrob. Agents Chemother.* 34:235–240 (1990).
12. E. Fattal, J. Rojas, L. Roblot-Treupel, A. Andremont, and P. Couvreur. Ampicillin-loaded liposomes and nanoparticles: Comparison of drug loading, drug release and *in vitro* antimicrobial activity. *J. Microencaps.* 8:29–36 (1991).
13. E. Fattal, M. Youssef, P. Couvreur, and A. Andremont. Treatment of experimental salmonellosis in mice with ampicillin-bound nanoparticles. *Antimicrob. Agents Chemother.* 33:1540–1543 (1989).
14. J. S. Weldon, J. F. Munnell, W. L. Hanson, and C. R. Alving. Liposomal chemotherapy in visceral leishmaniasis: An ultrastructural study of an intracellular pathway. *Z. Parasitenkd.* 69:415–424 (1983).
15. S. Majumdar, D. Flasher, D. S. Friend, P. Nassos, D. Yajko, W. K. Hadley, and N. Düzgünes. Efficacies of liposome-encapsulated streptomycin and ciprofloxacin against *Mycobacterium avium-M. intracellulare* complex infections in human peripheral monocyte/macrophages. *Antimicrob. Agents Chemother.* 36:2808–2815 (1992).
16. V. Guise, P. Jaffray, J. Delattre, F. Puisieux, M. Adolphe, and P. Couvreur. Comparative cell uptake of propidium iodide associated with liposomes or nanoparticles. *Cell. Mol. Biol.* 33:397–405 (1987).
17. P. Couvreur, M. Roland, and P. Speiser. Biodegradable submicroscopic particles containing a biologically active substance and compositions containing them. U.S. Patent No. 4.329.332 (1982).
18. S. Henry-Michelland, M. J. Alonso, A. Andremont, P. Maincent, J. Sauzières, and P. Couvreur. Attachment of antibiotics to nanoparticles: Preparation, drug release and antimicrobial activity *in vitro*. *Int. J. Pharm.* 35:121–127 (1987).
19. T. B. Vree, Y. A. Hekster, A. M. Baars, and E. Van der Kleijn. Rapid determination of amoxycillin (Clamoxyl) and ampicillin (Penbritin) in body fluids of many by means of high-performance liquid chromatography. *J. Chromatogr.* 145:469–501 (1978).
20. O. Balland, H. Pinto-Alphandary, S. Pecquet, A. Andremont, and P. Couvreur. Intracellular uptake and activity of ampicillin-

loaded nanoparticles on murine macrophages infected by *Salmonella typhimurium J. Antimicrob. Chemother.* (in press).
21. R. Bacallao, M. Bomsel, E. H. K. Stelzer, and J. De Mey. Guiding principles of specimen preservation for confocal fluorescence microscopy. In J. B. Pawley (ed.), *Handbook of Biological Confocal Microscopy*, Plenum Press, New York and London, 1990, pp. 197–205.
22. V. Lenaerts, P. Couvreur, D. Christiaens-Leyh, E. Joiris, M. Roland, B. Rollman, and P. Speiser. Degradation of poly(isobutylcyanoacrylate) nanoparticles. *Biomaterials* 5:65–68 (1984).
23. R. Whitehouse, J. C. Benichou, and A. Ryter. Procedure for longitudinal orientation of rodshaped bacteria and the production of a high cell density of procaryotic and eucaryotic cells in thin sections for electron microscopy. *Biol. Cell.* 30:155–178 (1977).
24. B. Seijo, E. Fattal, L. Roblot-Treupel, and P. Couvreur. Design of nanoparticles of less than 50 nm in diameter. Preparation, characterization and drug loading. *Int. J. Pharm.* 62:1–7 (1990).
25. S. J. Douglas, L. Illum, and S. S. Davis. Particle size and size distribution of poly (butyl 2-cyanoacrylate) nanoparticles. II. Influence of stabilizers. *J. Colloid Interface Sci.* 103:154–163 (1985).
26. J. L. Grangier, M. Puygrenier, J. C. Gautier, and P. Couvreur. Nanoparticles as carriers for growth hormone releasing factor. *J. Control. Release* 15:3–13 (1991).